Advanced Materials Research Vol. 576 (2012) pp 406-412
© (2012) Trans Tech Publications, Switzerland
doi:10.4028/www.scientific.net/AMR.576.406

One-Dimensional ZnO Nanostructures by Wet-Chemistry Technique for Dye Sensitized Solar Cell Application

A.H. Yuwono*, N. Sofyan, S. Harjanto, D. Daneswara, A. Ferdiansyah, H. Dharma and O. Hammerstein

Department of Metallurgy and Materials, Faculty of Engineering, Universitas Indonesia, Jawa Barat 16424, Indonesia

*Corresponding author: ahyuwono@metal.ui.ac.id

Keywords: 1-D ZnO, nanorods, nanoflowers, PEG concentration, nanoseeding, DSSC

Abstract. In the current work, ZnO nanoflowers have been synthesized via sol-gel technique using a mixture of zinc-nitratetetrahydrate, ammonia and polyethylene glycol (PEG). Variation in PEG concentration and ammonia evaporation delay time was performed and the resulting nanoflowers have been investigated using x-ray diffraction (XRD) and scanning electronmicroscope (SEM). To explore the potential of the resulting ZnO nanorods, a prototype of dye sensitized solar cell (DSSC) has been fabricated. For this purpose, the nanorods were grown directly on conducting ITO substrates by nanoseeding technique. With a variation in nano seeding time for 2, 4 and 6 days, followed by hydrothermal process at 80^{o}C for 20 hours, ZnO nanorods with average diameter of 82, 332 and 1385 nm have been synthesized. The performance test showed the resulting open circuit voltage (V_{oc}) was increased from 398 to 486 mV when the diameter of ZnO nanorods increased from 82 to 332 nm. However, the V_{oc} decreased slightly to 456 mV when the nanorods further increased to 1385nm. The phenomenon is related to the interaction between the semiconductor oxide and the Ruthenium complex organic dye.

Introduction

Zinc oxide (ZnO) is a II-VI semiconductor, which has great potentials for electronic and optoelectronic devices as a result of its wide band-gap energy of 3.37 eV and large exciton binding energy of 60 meV at room temperature [1]. Over the past decades, one-dimensional (1D) nanostructures such as nanowires and nanorods have stimulated significant scientific interest due to their unique properties incomparison to bulk materials. The pioneering achievement by Iijima [2] in fabricating carbon nanotubes has increased research focus worldwide to synthesize 1D nanoscale materials of various elements and compounds. Moreover, since the first report of ultraviolet lasing from ZnO nanorods, substantial efforts have been devoted to the development of novel synthetic technique for 1D ZnO nanorods [3]. In general, the synthetic approaches can be classified into two categories, *i.e.* vapor phase process and solution phase route. As the high-temperature vapor-phase processes are expensive and energy-consuming [4], various solution-phase approaches to ZnO nanorods have recently attracted extensive interest because of their low growth temperatures and good potential for scale up [5].

In the present paper, we report our fabrication results of ZnO nanorods using zinc nitrate and ammonia as starting materials. In order to control the growth of ZnO nanorods, different concentration of organic polyethylene glycol (PEG) and ammonia evaporation delay time were involved during the reaction. The potential of the resulting nanostructure as the semiconductor oxide layer was further explored by fabricating a prototype of dye sensitized solar cell using ZnO nanorods grown directly on the conducting ITO substrates by nanoseeding technique.

Experiment Details

The synthesis procedure of ZnO nanorods in this work was adopted from the previous report by Zhang et al [6]. The route was started with dissolution of 5.23 gr zinc nitrate tetrahydrate ($Zn(NO_3)_2.4H_2O$) in 100 ml deionized water, followed by a thorough stirring for 2 hours. On the

All rights reserved. No part of contents of this paper may be reproduced or transmitted in any form or by any means without the written permission of TTP, www.ttp.net. (ID: 152.118.148.218-07/09/12,09:02:22)

other hand, 1 gram polyethylene glycol (PEG, M_w = 12000) was dissolved in 50 ml deionized water and stirred for 20 minutes at room temperature. Furthermore, 0.15 mol ammonia (NH_3) was added into this solution, followed by stirring for 10 minutes. The formation of ZnO nuclei was started by adding the second solution drop wise into the first solution with slow stirring process until the pH value of the mixture was ~10.5. Once this pH was obtained, the stirring process of the mixture solution was performed faster, accompanied by a heating process at 75^{o}C for 2 hours, resulting in white color precipitate. For comparison purposes, the PEG concentration added during the preparation of the second solution was also varied into 2 and 3 grams. It should be noted that for the above procedure, the cover of the beaker glass for the mixture solution was purposely open to enable the ammonia evaporation. The onset of ZnO nanostructure formation occurred at the first 1 hour, indicated by the change of solution from transparent to milky. Full-precipitate was completely obtained in the second hour, which was further filtered and rinsed 3 times with deionized water and ethanol to neutralize the remaining ions involved in the reaction. Finally, the white precipitate was dried at 60^{o}C in drying oven for 12 hours. Variation in the synthesis route for ZnO nanorods was also purposely performed with ammonia evaporation delay time. This was carried out by covering the beaker glass for reaction for 1 and 2 hours so that the ammonia could not evaporate instantaneously, and furthermore followed by normal heating process at 75^{o}C for another 2 hours to complete the formation of white precipitate.

For DSSC fabrication, the ZnO nanorods were grown directly on ITO substrates through nanoseeding route. The seeding solution was prepared by dissolving 6,8 grams zinc acetate dehydrate ($ZnCH_3COO.2H_2O$) and 1.83 grams ethanolamine ($NH_2CH_2CH_2OH$) in 40 ml 2-methoxyethanol (CH_3OCH_2-CH_2OH) followed by stirring for 2 hours at constant temperature of 60-70^{o}C. This homogeneous solution was held for 2, 4 and 6 days for nanoseeding to occur. These nanoseeding solutions were subsequently deposited onto conducting ITO substrates by spin coating with 4000 rpm for 60 sec. Furthermore, the nanoseed ZnO thin films was pre-heated at 175^{o}C for 10 min, and further heating at 300 and 400^{o}C for 10 minutes. After cooling process to room temperature, the coated ITO substrates were washed with deionized water, dried at room temperature and re-heated at 350^{o}C for 30 minutes.In order to convert the nanoseed to form ZnO nanorods, the growing solution was prepared by dissolving 0.1 mM zinc nitrate tetrahydrate ($Zn(NO_3)_2.4H_2O$) in 0.1 mM hexamethylenetetramine ($(CH_2)_6N_4$) with magnetic stirrer for 2 hours.Furthermore, this homogenous solution was put into aTeflon-lined stainless steel autoclave (Parr Molline, Illinois). ITO substrates, which have been coated with ZnO nanoseed were in horizontal position where the thin films face downside to facilitate the growth of ZnO nanorods by gravitation force. The autoclave and the sample were heated in oven at 80^{o}C for 20 hours. After cooling to room temperature, the ITO substrates were rinsed with deionized water, dried at room temperature and re-heated at 60^{o}C for 24 hours. The resulting ZnO nanorods were characterized by using X-ray diffraction (Bruker AXS θ-2θ diffractometer using Cu K-α radiation of 1.5406Å, operated at 40 kV, 40 mA) and scanning electron microscope (JEOL–JSM 6510LV).

Results and Discussions

Effect of PEG addition: Figs.1a-c are the SEM images of ZnO nanorods synthesized with PEG addition of 1, 2 and 3 grams under a constant ammonia evaporation. All the samples showed cluster-like nanoflowers where the individual nanorods protruded out from each center. Based on the image analysis, the average diameters of individual ZnO nanorods of the above samples were 158, 301 and 464 nm. The formation of ZnO nanorods is related to the role of PEG as template for the precursor absorption and furthermore facilitated the alignment mechanism anisotropically, following the chain-like structure of PEG molecules [7]. With respect to the increase of average diameter from 158 to 464 nm as a result of PEG addition from 1 to 3 grams (Fig. 1a and b), the current results confirm the investigation by Zhengquan *et al* [8] where the addition of PEG increased the intertwisting mechanism, which in turn resulting in ZnO nanorods of larger diameter. It has been found in the present work that the addition of 3 grams PEG was the maximum suitable condition for the formation of ZnO nanorods. This was confirmed by the addition of 5 grams PEG

resulted in the mixture solution of zinc nitrate and ammonia did not react to form ZnO nanorods, as indicated by the color of the reaction mixture remained transparent and no precipitate found until the heating process at 75^{o}C finished after 2 hours. In order to confirm the resulting inorganic phase and its crystallinity level, x-ray diffraction was performed on the samples with PEG addition of 1, 2 and 3 grams. (Fig.2). All the diffraction peaks at 2θ of 32.05, 34.71, 36.53, 47.72, 56.75 dan 63.26^{o} can be indexed as (100), (002), (101), (102), (110) and (103) crystal planes of wurtzite structure ZnO.

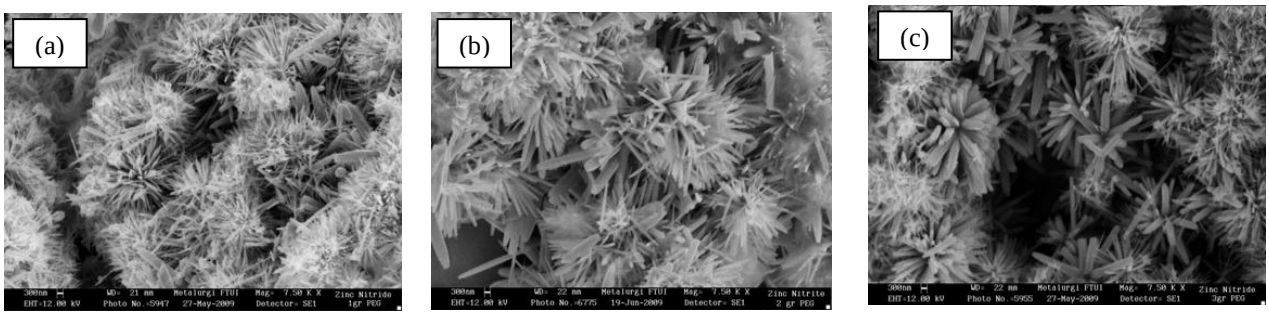

Fig. 1. SEM images of ZnO nanorods resulted from reaction between $Zn(NO_3)_2.4H_2O$ and NH_3 with addition of (a) 1; (b) 2; and 3 grams PEG.

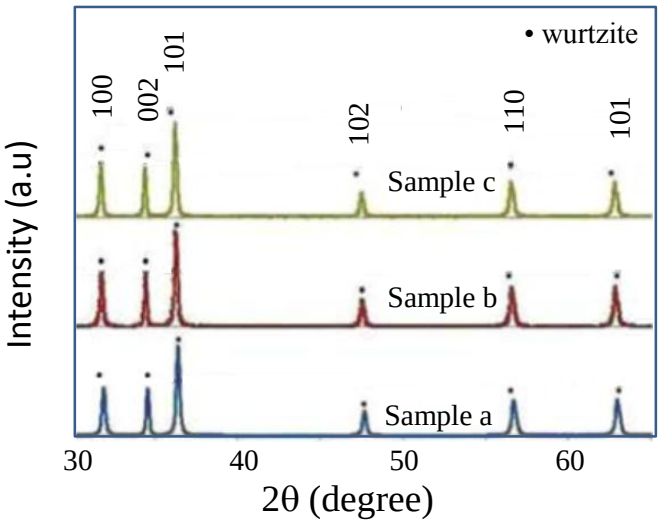

Fig.2. XRD traces of ZnOnanorods derived from $Zn(NO_3)_2.4H_2O$ and NH_3 with PEG addition of: (a) 1; (b) 2; and 3 grams.

The estimation of the crystallite size of wurtzite phase in nanorods was performed by using Scherrer's formula [9]. It should be noted that for the sake of calculation accuracy, broadening due to the non-uniform strain and the instrumental line width in the XRD apparatus have been excluded [10]. It was found that by addition of PEG from 1, 2 and 3 grams, the average crystallite size of wurtzite phase in the solid nanorods structure just slightly increased from 94.8 to 94.9 and finally 95.4 nm.

Effect of ammonia evaporation delay time: Figs.3a-c show SEM images of ZnO nanoflower samples with addition of 3 grams PEG without ammonia evaporation delay time (sample d) and those of 1 and 2 hour ammonia evaporation delay time (sample e and f, respectively). Based on the observation of the whole area of the samples, it was found that samples e and f provided more uniform distribution of nanorods structure in comparison to sample d. On the basis of image analysis, it was found that ZnO nanorods derived from the delay of ammonia evaporation for 1 hour have average diameter of 410 nm,which is smaller than that of without ammonia evaporation delay (464 nm). Further delay of ammonia evaporation for 2 hours has decreased the diameter of nanorods more significantly to 328 nm.

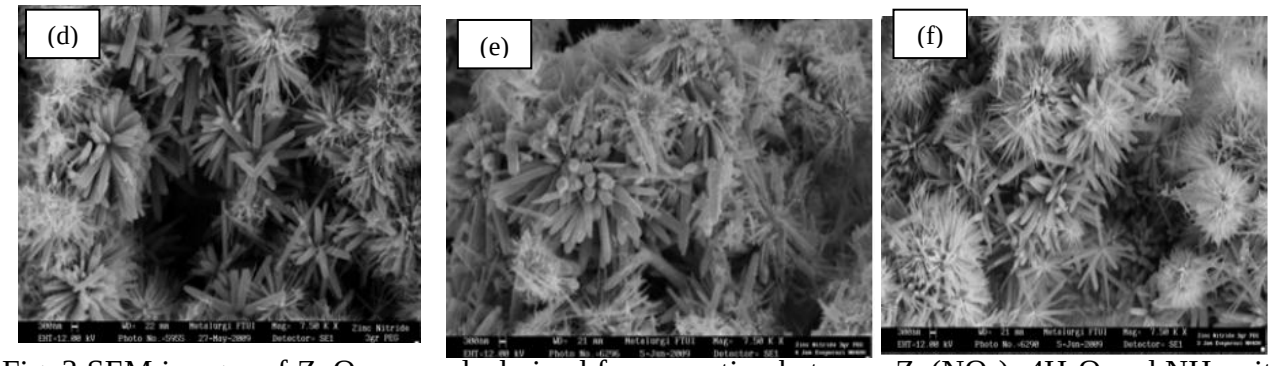

Fig. 3 SEM images of ZnO nanorods derived from reaction between $Zn(NO_3)_2.4H_2O$ and NH_3 with addition of 3grams PEG without ammonia evaporation delay time (sample d) and those of with 1 and 2 hour ammonia evaporation delay time (sample e and f).

X-ray diffraction was carried out for the three samples and the results reconfirmed that the resulting inorganic phase in nanorods was wurtzite ZnO (Fig. 4). Again, the crystallite size estimation by Scherrer's formula was performed and showed that the delay of ammonia evaporation has affected the average diameter and crystallite size in reverse direction. While this modification has decreased the average diameter of nanorods, the crystallite size of the resulting wurtzite phase inside the solid structure, however, has increased from 95.4, 121.5 and 166.6 nm for sample d, e and f, respectively. The crystallite size enhancement was expected to be due to the growth of ZnO nuclei to form a bigger wurtzite phase within smaller diameter constrain.

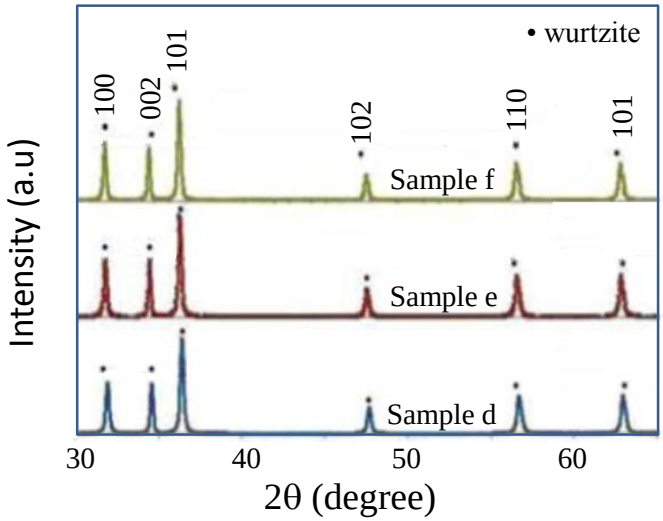

Fig.4 XRD traces of ZnO nanorods derived from reaction between $Zn(NO_3)_2.4H_2O$ and NH_3 with addition of 3grams PEG without ammonia evaporation delay time (sample d) and those of with 1 and 2 hour ammonia evaporation delay time (sample e and f).

Effect of nanoseeding time: Figs.5a-c are SEM images of ZnO nanorods derived from nanoseeding technique on ITO substrates with seeding time variation of 2, 4 and 6 days. With 2 days seeding time, the structure of ZnO phase was dispersed uniformly over the surface of ITO and existed as short nanorods in horizontal position (Fig. 5a). Subsequent increase of seeding time to 4 days, the nanorods started to connect each other, forming networks of larger nanorods (Fig. 5b). Further increase in seeding time up to 6 days (Fig. 5c) resulted in micro-size features dominated the ITO surface and overlapped each other. It can be seen that there also existed small branch nanorods growing out from these individual large rod-like structures. The image analysis results provided that the increase in nanorods diameter took place progressively from 82.33 nm with 2 day seeding time to 332.39 nm with 4 day, and finally grew further at microscale to 1384.78 nm with 6 day seeding time. This confirmed the effect of variation in time during seeding preparation to the growth of

nanorods upon the subsequent hydrothermal stage in autoclave at 80°C for 20 hours using zinc nitrate tetrahydrate and hexamethylenetetramine. In addition, the variation in seeding time also affected the difference in maximum-minimum diameter in comparison to the average value. The value increased from 7.57 to 12.43, and finally 26.86 % with the increase of seeding time from 2, 4 and 6 days. This data also shows that the increase of the average diameter in nanorods as the effect of longer seeding time was accompanied bya more variation in size among the ZnO nanorods under the same sample preparation condition.

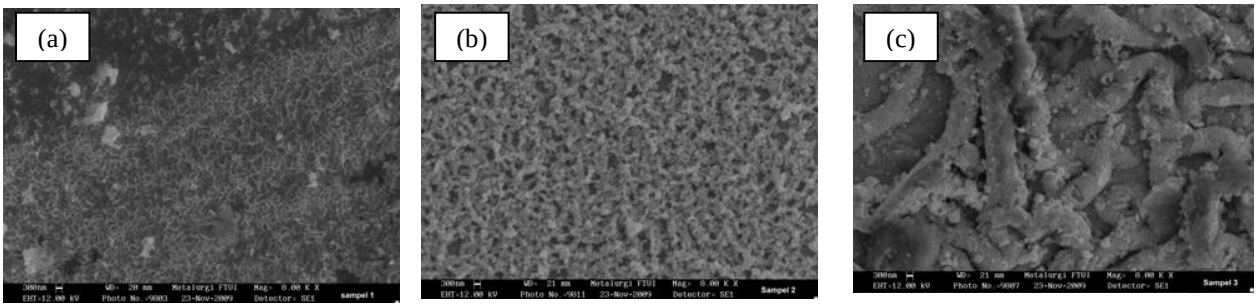

Fig. 5 SEM images of ZnO nanorods derived from hydrothermal process with nanoseeding time of: (a) 2; (b) 4 and (c) 6 days.

The open circuit voltage (V_{oc}) of DSSC fabricated by ZnO nanorods with various seeding time: The measurement of the open circuit voltage (V_{oc}) of DSSC fabricated by ZnO nanorods with various seeding time was carried under two conditions, *i.e.* dark with room light illumination and bright with focused illumination using LED light. The dark testing was purposely performed to confirm there is no short circuit voltage as indicated by low voltage during this minimum illumination. Figs. 6a and b present the results of the above measurement as a function of average diameter of ZnO nanorods.

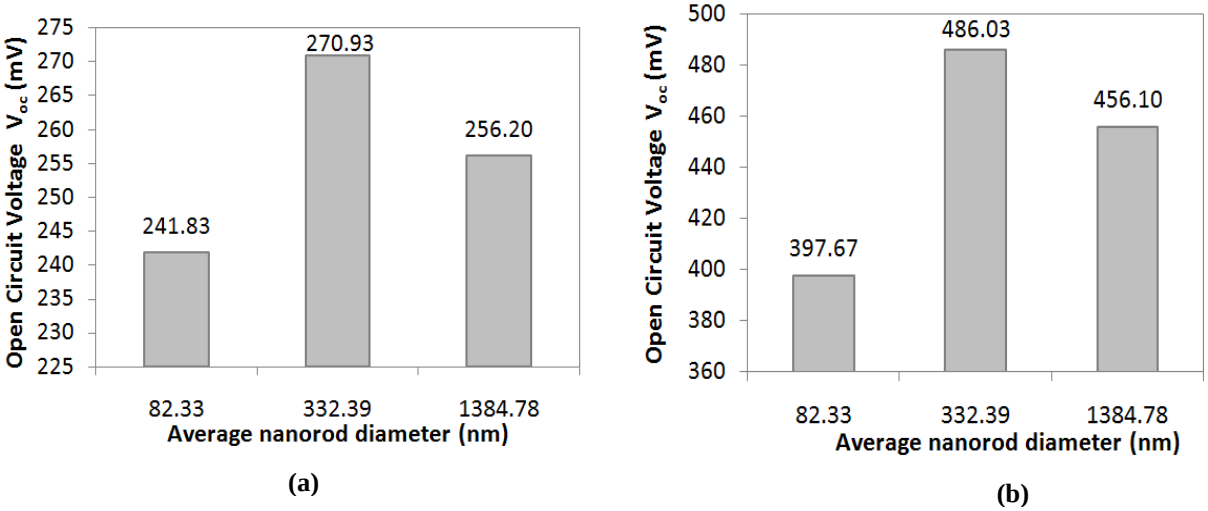

Fig. 6. The results of V_{oc} measurement under (a) dark and (b) illumination of DSSC as function of ZnO nanorods diameter derived from hydrothermal process with nanoseeding time of 2, 4 and 6 days.

Under dark illumination (Fig. 6a), the V_{oc} value increased from 241.83 to 270.93 mV when the ZnO nanorods diameter used in fabrication of the DSSC increased from 82.33 to 332.39 nm. However, further increase in nanorods diameter up to 1384.78 nm adversely decreased V_{oc} value down to 256.20 mV. Similar trends was also demonstrated when bright illumination was carried out (Fig. 6b) but with higher V_{oc} value, *i.e.* there was an increase from 397.67 to 486.03 mV when the ZnO nanorods diameter increased from 82.33 to 332.39 nm, followed by a slight decrease to 456.10

mV when bigger ZnO nanorods of 1384.78 nm in the DSSC. The optimum V_{oc} value, both at dark and bright illumination, obtained by the DSSC fabricated with ZnO nanorods of 332.39 nm was related to the ability of Ru-N3 dye solution to penetrate to the pores created by nanorods structure. This dye solution contains ruthenium element, which has average size between 10 to 20 nm [11]. For the DSSC fabricated with nanorods of 82.33 nm in diameter (Fig. 5a), there was open space, which is only about four times larger than the size of ruthenium element itself to enable the ruthenium complex dye to penetrate to the solid structure. As a consequence, this situation made the interaction between the sensitizing dye and the semiconductor oxide is not intensive yet. As widely accepted, one of governing factors to determine the performance of DSSC is the ability of the dye solution to inject the excited electrons, as a result of photon absorption, to the conduction band of semiconductor oxide. With a bigger open space provided by ZnO nanorods with average diameter of 332.39 nm (Fig. 5b), the open space is about 15 times than the size of ruthenium element. Indeed, this enabled more pronounced interaction between the dye solution and semiconductor oxide, resulting an increase in V_{oc} up to 486.03 mV (under bright illumination). However, with much bigger ZnO nanorods of 1384.78 nm in diameter, the value of V_{oc} decreased adversely. This can be understood since these bigger nanorods have many small branch nanorods growing out from these individual large rod-like structures (Fig. 5c). This caused the whole structure became denser, resulting in difficulty for the dye solution to penetrateto pore structure in reaching the surface of semiconductor oxide. As a result, the decrease in V_{oc} value in the fabricated DSSC was obviously observed.

Fig.7 presents the comparison between the V_{oc} value obtained by the DSSC prototype fabricated with ZnO bulk and nanorods. It should be noted that the ZnO bulk DSSC was fabricated by using the standard procedure where the ZnO powder was prepared in the form of paste, which was further spread over the ITO substrate via doctor blade technique.

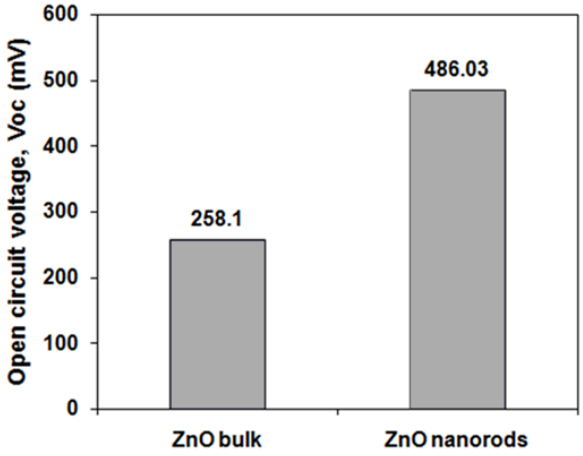

Fig. 7. The comparison between the V_{oc} of the DSSC prototype with ZnO bulk and nanorods.

It is shown that the DSSC with ZnO nanorods was able to provide the V_{oc} value of 486.03 mV, which is almost two times higher than that of ZnO bulk *i.e.* 258.10 mV. This demonstrates that the nanorods structure can facilitate synergistic condition towards the interaction between the sensitizing dyesolution and semiconductor materials; both are the governing factors for DSSC performance. The uniform distribution of pore structure created by ZnO nanorods in Fig. 5b enabled more pronounced dye penetration which in turn assisted in the injection process of excited electrons to the conduction band of ZnO. In addition, although the nanorods structure in this work was not ideal yet since the growth was still in the horizontal direction over the substrate surface; however there was a possibility that this characteristic already facilitated the ballistic effect of electron, providing more straightforward electron trajectory in comparison to the tortuous path resulted from the conventional nanoparticles.

Conclusions

The diameters of individual nanorods in ZnO nanoflowers under the current investigation were affected by PEG concentration and ammonia evaporation delay time. The optimum open circuit voltage (V_{oc}) value of 486.03 mV was obtained by the DSSC fabricated with ZnO nanorods of 332.33 nm derived from nanoseeding technique for 2 days. It was related to the most suitable pore size which enabled the dye solution to penetrate to the ZnO nanorods structures and played important role in the injection process of excited electrons to the conduction band of ZnO.

Acknowledgements

The authors would like to thank the financial support from Directorate of Research and Community Services-Universitas Indonesia (DRPM-UI) through Riset Unggulan Universitas Indonesia (RUUI) Year 2011, with contract no. No. 1367/H2.R12/PPM.00.01Sumber Pendanaan/2011.

References

[1] C.M. Jin, A. Tiwari, R.J. Narayan, Ultraviolet illumination enhanced photoluminescence effect in zinc oxide thin films, J.Appl.Phys. 98 (2005) 1-5.

[2] S. Ijiima, Helical microtubules of graphitic carbon, Nature 354 (1991) 56–58.

[3] M. H. Huang, S. Mao, H. Feick, H. Yan, Y. Wu, H. Kind, E. Weber, R.Russo, P. Yang, Room-Temperature Ultraviolet Nanowire Nanolasers, Science 292 (2001) 1897-1989.

[4] C. H. Chia, T. Makino, K.Tamura, Y. Segawa, M. Kawasaki, A. Ohtomo, H. Koinuma, Confinement-enhanced biexciton binding energy in ZnO/ZnMgO multiple quantum wells, Appl. Phys. Lett. 82 (2003) 1848-1850.

[5] B.Liu, H. C. Zeng, Room Temperature Solution Synthesis of Monodispersed Single-Crystalline ZnO Nanorods and Derived Hierarchical Nanostructures, Langmuir 20 (2004) 4196-4204.

[6] H. Zhang, J.F. Feng, J Wang, M. Zhang, Preparation of ZnO nanorods through wet chemical method, Matter. Lett. 61 (2007) 5202-5205.

[7] X.Zhou, D.Zhang, Y.Zhu, Y.Shen, X. Guo, W. Ding, Y.Chen, Mechanistic investigations of PEG-directed assembly of one-dimensional ZnO nanostructures, J. Phys. Chem. B 110 (2006) 25734–25739.

[8] Z.Li, Y.Xiong, Yi Xi, Selected-Control Synthesis of ZnO Nanowires and Nanorods via a PEG-Assisted Route, Inorg. Chem., 42 (2003) 8105–8109.

[9] B.D. Cullity: Elements of X-ray Diffraction, 2nd ed., Addison-Wesley Reading, Massachusetts, 1978.

[10] C. Suryanarayana, M.G. Norton, X-Ray Diffraction: A Practical Approach, Plenum Press, New York, 1998.

[11] M., Mohammad Hashim A, Al-Maamory M, Highly Conductive and Transparent ZnO Thin Films Prepared by Spray Pyrolysis Technique, Mat. Chem. Phys, 99 (2006) 382-387.

View publication stats